J Solid State Electrochem (2011) 15:1217–1225
DOI 10.1007/s10008-010-1191-9

ORIGINAL PAPER

Study of $LiFePO_4$ synthesized using a molten method with varying stoichiometries

Benjamin Daheron · Dean D. MacNeil

Received: 23 May 2010 / Revised: 28 August 2010 / Accepted: 4 September 2010 / Published online: 18 September 2010

Abstract The synthesis of $LiFePO_4$ from a melt cast of Li_2CO_3, $FePO_4$, and carbon precursors at 1,000 °C was recently reported. The results indicate that it could be a competitive technique for the large-scale production of $LiFePO_4$. This paper focuses on particle size reduction and non-stoichiometric synthesis of $LiFePO_4$. The particles size was reduced using a planetary mill that is available in most research laboratories where the milling time and milling media were varied to obtain the best electrochemical results. In addition, the electrochemical performance of $LiFePO_4$ products synthesized from $FePO_4 + x/2\,Li_2CO_3 + C$ (sequentially varying the amount of x) at 1,000 °C has also been measured. The stoichiometric $LiFePO_4$ product shows the best capacity, while the off-stoichiometric material demonstrates different levels of impurities that have an effect on the performance of the material. The results indicate that adequate capacity at low discharge rates can be obtained using standard milling techniques, but, in order to obtain material from a melt cast synthesis that provides higher performance at faster discharge rates, a further particle size reduction will be required.

Keywords Melt casting · $LiFePO_4$ · Particle size reduction · Non-stoichiometric synthesis

Introduction

Many of the current and emerging electric vehicle options are based on an energy storage mechanism, which involve batteries. Lithium-ion batteries are considered the most suitable choice in battery chemistry as they store more energy per volume than any other portable rechargeable battery system available [1]. Researchers have been concentrating on finding new materials that offer better performance, lower costs, and increased safety compared with the electrode materials found within the first lithium-ion batteries, namely $LiCoO_2$ and graphite. The active electrode materials of these batteries, in their charged state, have been shown to partake, when abused, in exothermic reactions at elevated temperatures. Temperatures in excess of 700 °C have been measured [2], and many cases of laptop fires have been reported [3]. It has been previously shown that the major thermal instability within Li-ion batteries is due to the release of oxygen from the $LiCoO_2$ cathode that causes the combustion of the liquid organic electrolyte [4]. This reaction can be described via autocatalytic kinetics and results in a rapid temperature rise, followed closely with the explosion of the cell [5].

Lithium iron phosphate ($LiFePO_4$) is considered a very promising active material for the cathode of large EV-sized batteries. The material, belonging to the olivine family of minerals, can provide high theoretical specific capacity (170 mAh/g) [6], improved thermal stability [7], and the possibility of lower costs. The high theoretical capacity is due to the possibility of electrochemically removing all of the lithium from the olivine structure. In addition, the inductive effect of the covalent P–O–Fe bonding within the olivine structure gives rise to a high discharge voltage of ~3.4 V versus Li^+/Li [6]. The improved thermal stability of $LiFePO_4$ is due to the stability of the discharged material, $FePO_4$, towards oxygen release. This eliminates the combustion of the organic electrolyte at elevated temperature. Finally, the lower cost of $LiFePO_4$ is due to the use of iron as redox active center as compared with more

B. Daheron · D. D. MacNeil (✉)
Département de chimie, Université de Montréal,
Montréal, QC H3T 1J4, Canada
e-mail: dean.macneil@umontreal.ca

expensive elements such as nickel and cobalt. Unfortunately, the conductivity of $LiFePO_4$ is fairly low. This necessitates the synthesis of small particles and the coating of the particles with a conductive carbon [8], which ultimately reduces the energy density of the material.

A variety of syntheses have been proposed for $LiFePO_4$, including solid-state reactions and solvent-assisted syntheses. The main disadvantage of the solid-state syntheses is the use of fairly expensive precursors, such as $FePO_4$ or FeC_2O_4 [9]. In comparison, solvent-assisted methods necessitate a large capital-intensive manufacturing process [10]. Our group has recently reported on the synthesis of $LiFePO_4$ in a molten-state [11, 12]. This synthesis technique allows the use of commodity-based reagents for the iron and phosphorus source, process simplicity as well as a complete and rapid reaction at equilibrium within a liquid state. Synthesis within a molten state combines ideal liquid-phase reaction kinetics and short dwell times to provide a product with high material density using a simple process method. Our initial papers concentrated on the development of the synthesis method, characterizing the product and investigating its electrochemical performance. The main disadvantage of the method was the necessity to reduce the particle size of the molten product due to the large crystals obtained after the slow cooling of the product. Our previous report concentrated on the use of a continuous-flow agitator bead mill that is not readily available within academic laboratory settings. In this work, electrochemically active $LiFePO_4$, synthesized via a molten procedure, is prepared by the use of commonly available laboratory milling mills and various sized milling media to improve the applicability of the synthesis method for the preparation of electrode material. In addition, we characterize the effect of changing the precursor stoichiometry during the molten synthesis on the performance of the product.

Experimental

Preparation

Melt casting was performed within an airtight box furnace under an Ar protection following the procedure described in Ref. [11]. Briefly, stoichiometric amounts of $FePO_4 \bullet 2H_2O$ (Buddenheim KG, Germany) and Li_2CO_3 (Limtech, Québec) were combined with 25 mol% of graphite powder (Superior Graphite ABG1045). The mixture was then placed in a graphite crucible and heated to 1,000 °C for 1 h. After cooling to room temperature, the ingot obtained from the synthesis was crushed and then ground in a mortar with a pestle to a powder. Five grams of this powder was then placed in a planetary mill (Fritsch) with a five times excess of iso-propyl alcohol (IPA) for suspension. The planetary mill used a 250-mL Syalon (Si_3N_4) container containing ~100 g of either 27-, 10-, or 5-mm Syalon media. A variety of milling times were used, and they are described in this work. The mill operated at a speed of roughly 600 rpm.

Characterization

X-ray analyses of the synthesized materials were performed on a Bruker D8 advance diffractometer using Cu Kα radiation. The phase purity and lattice parameters of the sample were calculated using the Topas Rietveld refinement program using the *Pnma* space group. The morphology of the powder was examined by scanning electron microscopy (SEM, Hitachi S-4300). The particle size of the powders used in this evaluation were analyzed using a Microtrac S3500 (Microtrac Inc.) and estimated from the SEM images. The thermogravimetric analysis (TGA) and differential scanning calorimetry (DSC) analyses were performed using a SDT600 from TA instruments coupled with a mass spectrometer (Pfeiffer) for off-gas analysis. The heating rate was 10 °C/min, and the experiments were performed with a flowing He carrier gas. The specific surface area of the sample was measured by the Brunauer, Emmett, Teller (BET) method (Micromeritics Gemini 2380). Carbon content for the samples was analyzed using a LECO C, S analyzer (LECO-SC632).

Electrochemical evaluation

To evaluate the material as a potential cathode material for Li-ion batteries, the milled powder was mixed with β-lactose (5 wt.%) in IPA. The suspension is mixed with the help of a Rotovap and an ultrasonic bath. After removal of the solvent, the dried powder is then heated to 700 °C for 3 h under a continuous N_2 flow. The sample is then passed through a 45-μm sieve to obtain a homogenous powder. Electrochemical evaluation of the samples was performed by combining 10 wt.% of a conductive carbon (Superior Graphite EBN1010) and 10 wt.% polyvinylidene difluoride (5 wt.% in *n*-methyl pyrrolidone (NMP)) with the electrode powders. An extra portion of NMP was added to the mixture to form a slurry, which was then mixed overnight in a roller mill. The slurry was then coated on a piece of carbon-coated Al foil. The electrode was dried overnight at 60 °C under dry air. The next day, 13-mm diameter disks were punched for cell assembly in standard 2032 coin-cell hardware (Hohsen) with a single lithium metal foil used as both counter and reference electrode and a Celgard-2200 separator. Cells were assembled in an argon-filled glove box using 1 M $LiPF_6$ in ethylene carbonate/diethyl carbonate (3:1 by vol) electrolyte (UBE).

Electrochemical evaluations were performed at 25 °C on a VMP electrochemical station (Biologic, France) with

EClab software using a potentiodynamic cycling with galvanostatic acceleration analysis (PCGA) [13]. In this test, the potential of the cell is increased stepwise by 20.1 mV between 3.0 and 3.7 V versus Li, while the resultant current is recorded every 0.020 mAh. The potential at each step is held for 60 min or until the measured current falls below 10 μA at which point the potential is varied for the next step. This cycle was repeated four times. After the PCGA test, the cell is placed under galvanostatic cycling conditions at a rate of C/10 between 2.2 and 4.0 V versus Li/Li^+. The C/10 current value is determined by the total capacity obtained during the PCGA analysis.

Results and discussion

Optimal particle size

It has been shown previously that heating $FePO_4.2H_2O$, Li_2CO_3 and graphite to 1,000 °C results in the following reactions [11]: loss of water at ~200 °C, loss of CO_2 from either Li_2CO_3 decomposition, or a reaction initially at 400 °C and then from the carbothermic reduction of Fe^{3+} to Fe^{2+} (from ~650 to 900 °C). This was followed by the melting endotherm of $LiFePO_4$ at ~960 °C. After cooling this sample in an Ar atmosphere, one obtains an ingot with large visible green crystals that can extend over several centimeters. An XRD investigation of the sample obtained through a 1 to 0.5 molar combination of $FePO_4$ and Li_2CO_3 is shown in Fig. 1a. The main reflections can be indexed on an orthorhombic olivine-type structure with the *Pnma* space group. The sample is free of major impurities, but a minor amount is visible near 25° and is likely from the presence of a small amount of $Fe_3(PO_4)_2$ in the sample. No Fe_2P has been detected in any of the samples synthesized. This is surprising due to the presence of 25 mol% graphite in the precursors during synthesis. Typically, the presence of a large amount of carbon during synthesis leads to the reduction of $LiFePO_4$ to Fe_2P [9]. This demonstrates the feasibility of producing $LiFePO_4$ in the molten state at 1,000 °C without significant decomposition of the product. The XRD investigation cannot preclude the absence of nanocrystalline or amorphous products in the final product. Our previous work [12] has shown that when naturally occurring triphylite is melted, the impurities agglomerate together into larger grain boundaries within the sample. This agglomeration would discount the formation of nanocrystalline impurity domains throughout the sample, and the slow cooling of the sample hinders the formation of amorphous domains. We believe that any major impurities would be visible by XRD, but further investigations using local probes (such as Mössbauer and magnetic measurements) will be the subject of further work from our group. In spite of this, Rietveld refinement of the as-synthesized $LiFePO_4$ crystals gave a unit cell volume of 291.1 $Å^3$, which is approximately the same as that found in literature [14]. Thus, due to the slow cooling of the samples synthesized in the molten-state, the product will crystallize into a well-ordered olivine structure. It is believed that the solidification process will have a significant effect on the formed crystal structure, microstructure, and phase purity of the molten sample. This will be examined in further investigations from our group.

Our previous work, on samples obtained using the molten synthesis, has shown that particle size reduction is required in order to (a) reduce the mass transfer resistance within the $LiFePO_4$ particle and (b) to obtain adequate electrochemical performance. Figure 1b presents the XRD profile of the sample shown in Fig. 1a except that the sample was subjected to milling within a planetary mill for 180 min using 10-mm Syalon media. Clearly, the milling procedure does not introduce any impurity to the sample, but the crystallites sizes within the sample are diminished due to the increase in peak width and loss of peak intensity. Obtaining a small average particle size is critical for optimal electrochemical performance of $LiFePO_4$ synthesized from a molten procedure. In this paper, we have concentrated on using a planetary mill, which is common to most laboratories working on battery materials, to reduce particle size. In planetary mills, the difference in speed between the grinding media and grinding jar produces an interaction between frictional and impact forces which

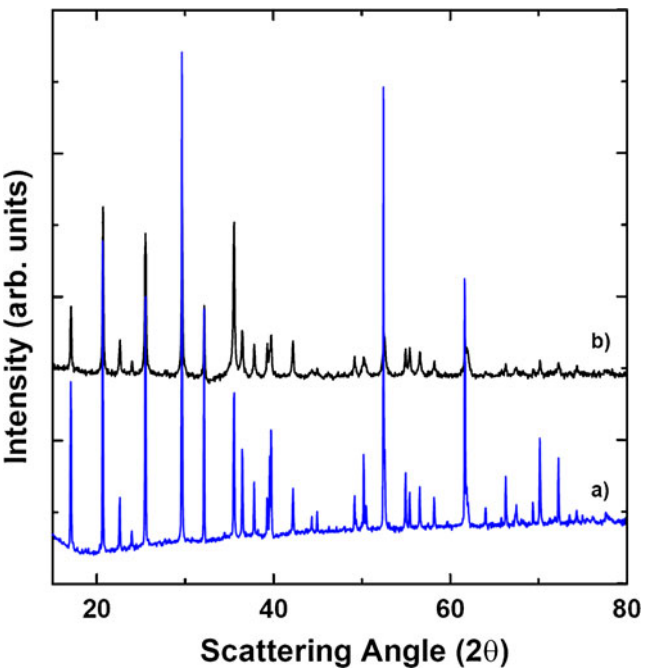

Fig. 1 X-ray diffraction of $LiFePO_4$ (space group *Pnma*) product before (**a**) and after (**b**) milling for 180 min using 10-mm milling media

release high energy. The high-energy impacts of the grinding media and between the media and the walls of the grinding bowl result in the grinding of the sample. There are numerous parameters that can be tuned for planetary milling, such as the choice of grinding media, their size, and amount. In addition, the milling time, load (ball: sample mass), and rotation speed can affect grinding. In this report, we have limited our investigation to the use of Syalon (90% Si_3N_4) milling media and jars. This material is highly resistant to abrasion and limits the introduction of impurities into our sample. We have also concentrated on a wet milling process (milling in an IPA suspension) as dry milling is typically limited to a minimum particle size of ~20 μm. During our investigation, we used a ball mass of ~105 g independent of ball diameter, providing a sample to ball mass ratio of ~0.05. The mill operated at a rotation speed of ~600 rpm. The variables tuned during this investigation were the size of the milling media and the milling time. Table 1 presents the particle size and surface area of the various $LiFePO_4$ samples milled using the planetary mill with various sized milling media and milling time. It is clear that increasing the time of milling for the same sized milling media results in a smaller particle size and larger surface area for the sample. As the milling time increases the number of collisions within the milling container increases, grinding the particles to finer and finer sizes and exposing more and more surface. Reducing the size of the milling media also leads to smaller particle sizes due to an increase in the number of collisions.

Table 1 Size and surface area of $LiFePO_4$ particles milled under planetary milling conditions with the indicated milling media size and milling time

Milling media size (mm)	Milling time (min)	Median particle size (μm)	Surface area (m^2/g)
27	5	10.09	1.34
	45	8.48	2.28
	90	5.04	2.91
	135	7.78	3.27
	180	6.54	4.20
	240	3.57	4.26
10	45	3.27	2.96
	90	2.52	5.37
	135	2.52	5.94
	180	2.31	7.80
	240	2.75	7.43
5	5	6.54	2.15
	90	1.95	8.76
	135	2.52	10.57
	240	1.78	18.26

Figure 2 shows the SEM images of some of the milled powders and demonstrates that increased milling time results in a reduction in the particle size of the material. In addition, a smaller-sized milling media produce powder with lower particle sizes, more exposed surface, and a more homogenous particle size distribution as compared with larger milling media. Unfortunately, planetary milling cannot be used to accurately control the particle size or morphology of each particle due to the random nature of the milling/grinding process, but the average particle size (as determined by the particle size analyzers) demonstrates reduction with increased milling time and smaller media. Simplistically, the milling process results in the destruction/milling of the larger particles, leaving the smaller particles untouched. The morphology of the sample also varies with milling time. The initial samples contain, for the most part, large rectangular-shaped crystallites with well-defined and smooth faces providing a lower surface area. As this product is milled for a longer period of time, the large crystallites get reduced and the morphology becomes less well-defined and more fractured, resulting in an increase in surface area. Interestingly, the samples do not show particle agglomeration during the milling process. Agglomerations would result in a severe drop in performance as some particles would be more difficult to access electrochemically due to a non-continuous electrical pathway towards the particle. In addition, agglomeration of the primary $LiFePO_4$ particles would affect the carbon-coating step (leaving an incomplete surface coverage of carbon for each individual particle within the agglomerate) that is necessary for optimal electrochemical performance.

The electrochemical behavior within lithium batteries of these various milled samples was then tested. Initially, the products were subjected to a carbon-coating procedure involving the thermal decomposition of β-lactose (10 wt.%) at 700 °C under a N_2 atmosphere. This carbon-coating procedure has been shown to eliminate the particle growth of the precursor that normally occurs during high temperature annealing of a non-coated sample [12]. In addition, carbon-coating smoothes out the morphology of the milled product, making the material easier to pack and giving it a more uniform shape. The carbon content of each sample after treatment at 700 °C was found to be ~1%. This amount of coating typically results in good electrochemical performance for $LiFePO_4$ produced via a number of synthetic routes. Figure 3 presents the discharge capacity as a function of cycle number and milling media size for many of the carbon-coated powders of Table 1. All milled materials show fairly good capacity retention with respect to cycle number (except for the large particles obtained from grinding in the mortar and pestle), but an improved cycle life is obtained with electrodes from powders with a smaller particle size. The loss of capacity with increasing cycle number for the

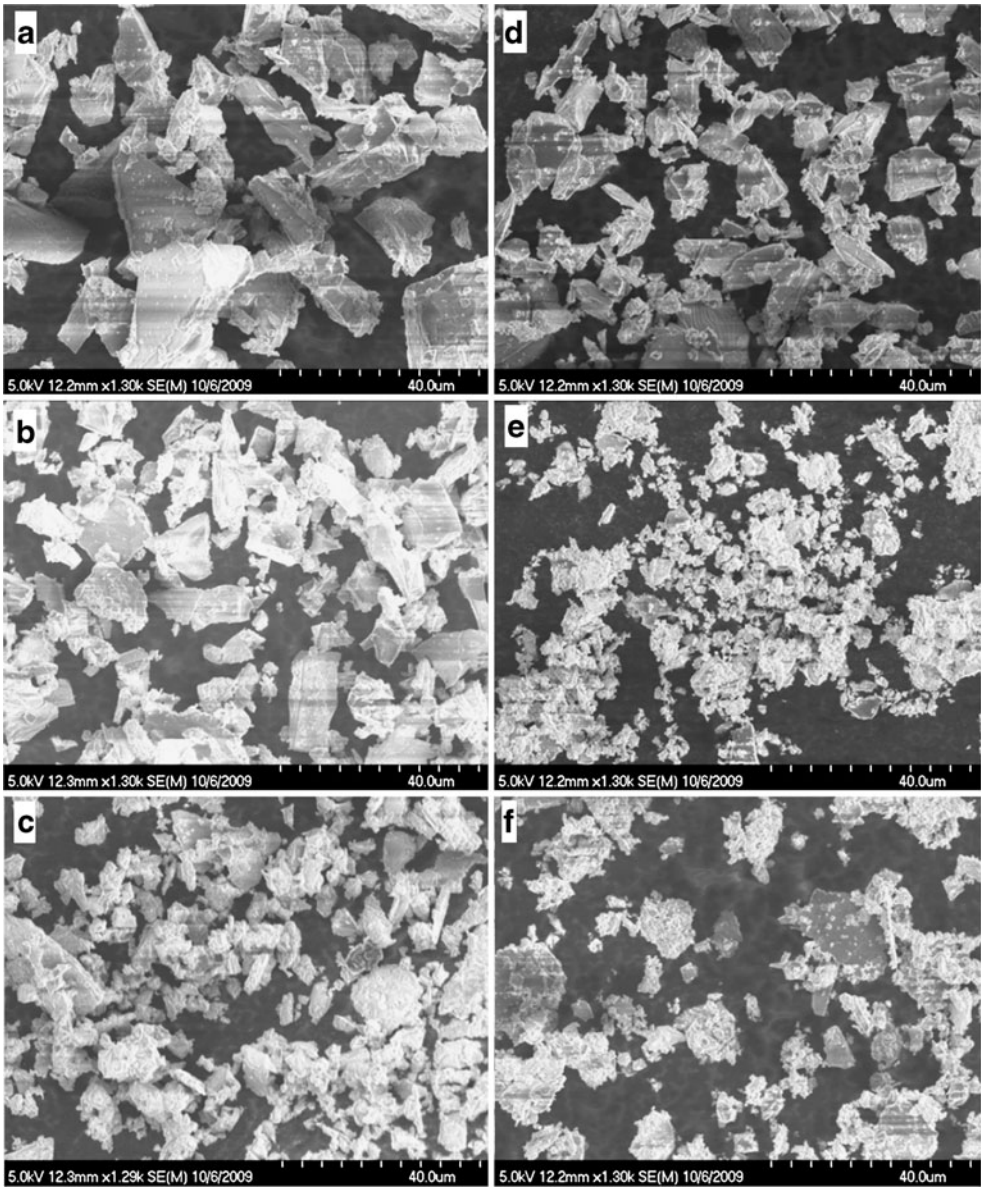

Fig. 2 SEM picture of $LiFePO_4$ milled with media either 27 mm (**a**–**c**) or 5 mm (**d**–**f**) in diameter for either 5 (**a**, **d**), 90 (**b**, **e**), or 240 min (**c**, **f**)

larger particles is likely due to the cracking of the particles during repeated cycling. This cracking results in the destruction of the carbon coating and loss of contact with the current collector leading to a loss in electrochemical activity. In comparison, the samples milled with the 5-mm media, which have the smallest particle size within this series of experiments, show capacities ~90% of theoretical values and improved cycle life due to lower strain on the particle as Li is removed and inserted repeatedly into the particle. This performance could be further improved with a lower particle size, but we are limited to milling media that is 5 mm in diameter for the planetary mill. A different milling technique has been shown to obtain smaller particle sizes and improved performance for molten $LiFePO_4$ sample to what is presented in Fig. 3, but the milling technique is not readily available in research laboratories [12].

Figure 4 presents a comparison of the PCGA response for the 10-mm media milled at 45, 135, and 240 min. Clearly, the electrochemical process is improved for the material with the lower particle sizes. This improvement is attributed to the decrease in resistive losses as the particle size of $LiFePO_4$ decreases. Within the battery electrode, ambipolar diffusion takes place where electron and ion diffuse together. As the particle size is reduced, diffusion length is reduced ($t=L^2/D$) and polarization effects can be minimized. The PCGA experiment demonstrates a more efficient insertion and de-insertion of Li within the structure as particle size is reduced, and this can have beneficial effects on the rate performance of the cell. With the above study, we have determined the optimal laboratory milling procedure for $LiFePO_4$ synthesized via the molten process. The ingot obtained from the synthesis is first crushed by

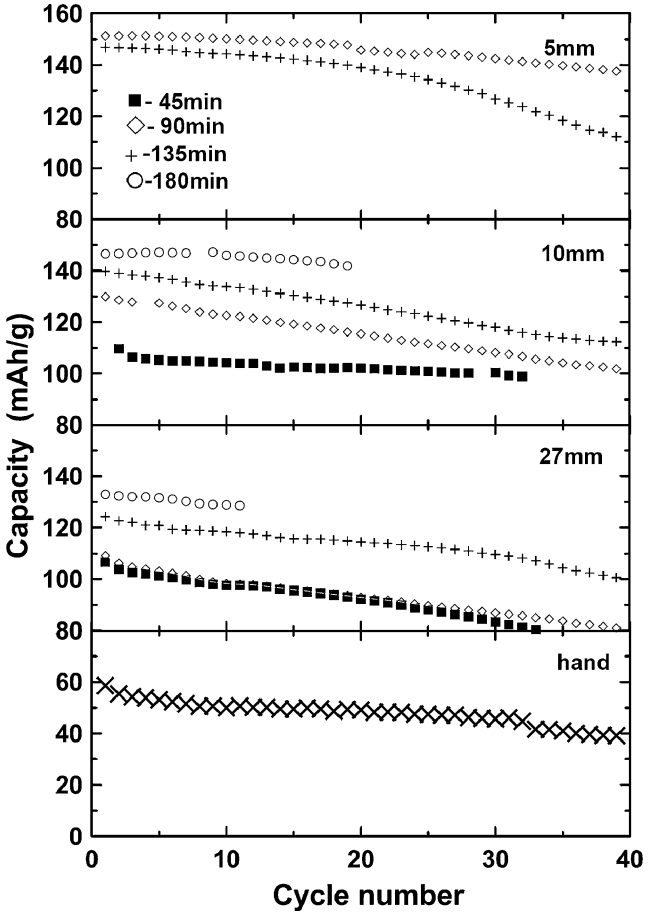

Fig. 3 Discharge capacity versus cycle number of $LiFePO_4$ synthesized using a molten method and subsequently milled either by hand or in the planetary mill for the indicated length of time

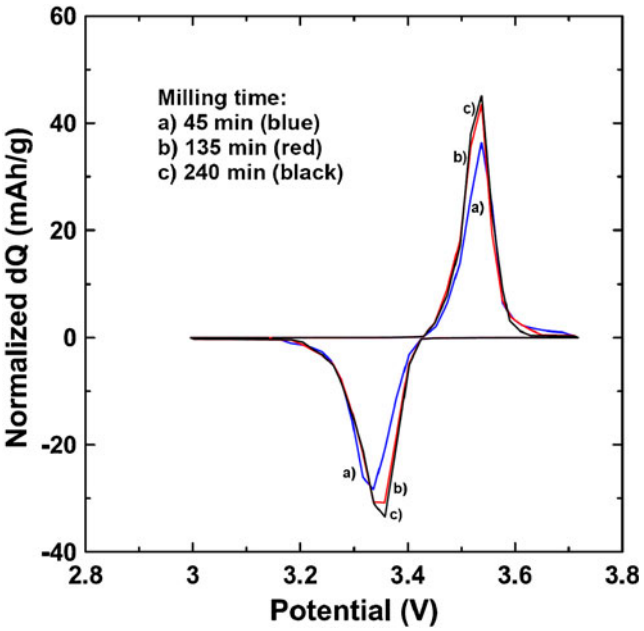

Fig. 4 Potentiodynamic cycling with galvanostatic acceleration (PCGA) response of the third charge/discharge cycle of $LiFePO_4$ milled with 10 mm media at the indicated time. Stepwise potential scans, 20.1 mV; current limits, 10 μA. Room temperature

hand and then transferred to a Syalon milling jar with 25 mL IPA as a mixing solvent. Approximately 100 g of 5-mm Syalon media beads are added, and the mixture is placed on the planetary mill for 90 min operating at a speed of 600 rpm.

Stoichiometry

In our previous studies on $LiFePO_4$ from a molten process, we concentrated on the investigation of the synthesis and characterization of the material from various precursors and obtaining optimal electrochemical performance using a continuously fed wet mill for particle size reduction. There has been a recent report in the literature that showed that non-stoichiometric coatings on $LiFePO_4$ can provide significant increases in rate capability [15]. Although this report is vigorously debated [16, 17], the molten synthesis method provides an excellent tool to investigate this area by simply melting different non-stoichiometric mixtures of precursors. Our previous report on melting naturally occurring triphylite suggested that any non-stoichiometric reactants are found outside the olivine structure as impurities in grain boundaries. In this experiment, we will confirm this observation and investigate its effect on the electrochemical performance of the material.

Figure 5 presents the XRD spectra of all samples synthesized through the desired combination of $FePO_4 + x/2\,Li_2CO_3 + 1/4\,C$. Each sample was mixed in the

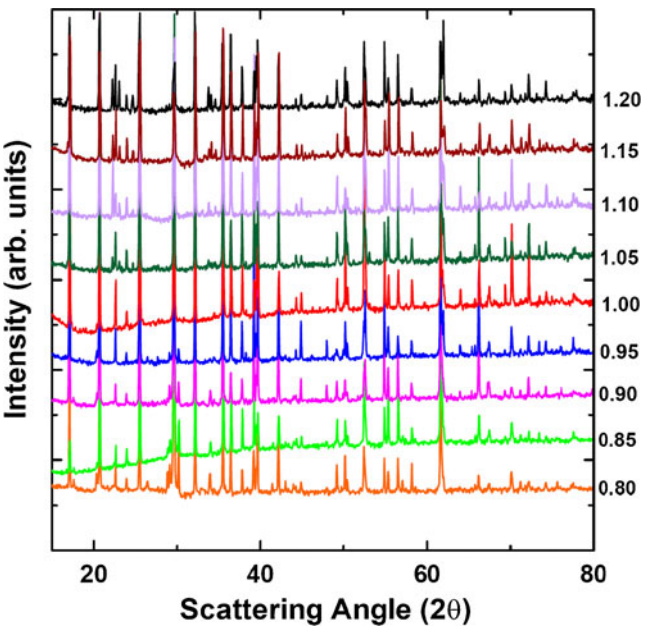

Fig. 5 X-ray diffraction of the products synthesized from $FePO_4 + x/2\,Li_2CO_3 + 1/4C$ at 1,000 °C at indicated value of x

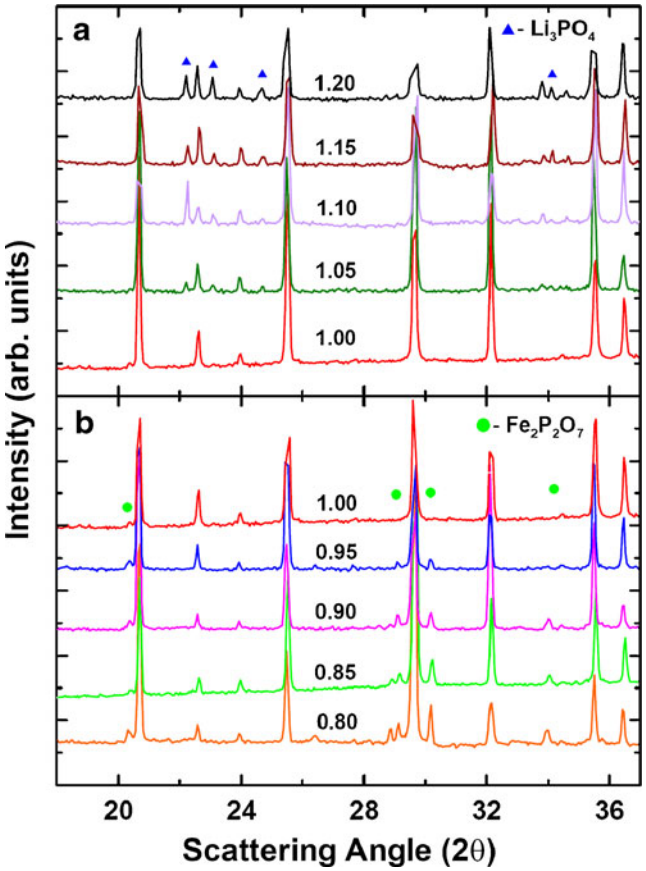

Fig. 6 X-ray diffraction of the products synthesized from $FePO_4 + x/2\,Li_2CO_3 + 1/4C$ at 1,000 °C for x=0.8 to x=1 in **a** and x=1 to x=1.2 in **b**. The main impurity is indicated in the respective figure and $LiFePO_4$ was refined on the *Pnma* structure

appropriate ratios and heated to 1,000 °C in a graphite crucible for 1 h under an Ar atmosphere. After cooling, the sample ingot was removed and crushed by mortar and pestle for X-ray analysis. We have been successful in producing pure $LiFePO_4$ for our x=1 sample, while samples with $x \neq 1$ contain varying amounts of impurities. To clearly view the impurities, Fig. 6 highlights the regions within the diffraction spectra that identify the impurities present with in the sample. When $x<1$ during the synthesis (Fig. 6a), the impurities found within the sample are rich in iron or phosphate (such as $Fe_2P_2O_7$), while for $x>1$ (Fig. 6b) the impurities are rich in Li (such as Li_3PO_4). Table 2 provides a summary of the results of these syntheses and the fittings using the *Pnma* space group. Some of the interesting results show that the volume obtained from $LiFePO_4$ is about 291 $Å^3$ in every case. This indicates that in each case, pure $LiFePO_4$ material is produced regardless of the amount and nature of the impurity. The variation within the calculated unit cell volumes is due to the impurities that affect our ability to obtain accurate fittings for the various diffraction spectra. Interestingly, there is no indication of any Fe_2P within any of the samples. Fe_2P is typically found when there is a high reducing environment and high temperatures, and has been used to explain the high rate capability found in certain so-called doped $LiFePO_4$ samples [9]. Further experiments involving an increase in the amount of the carbon introduced within the sample did not result in the production of any Fe_2P material. This demonstrates, contrary to what is commonly believed, that crystalline Fe_2P is not always produced at high temperatures under reductive conditions, but we cannot exclude that either an amorphous or nanocrystalline Fe_2P, not visible via our XRD investigation, can form under these conditions. Overall, it appears that the crystallization from the melt is controlled by phase diagram rules and the stoichiometry of the reactants used.

A DSC analysis (Fig. 7) of all the samples indicates clearly the effect that the impurities have on the melting point of $LiFePO_4$. As the concentration of impurities within the sample increase, the melting point of $LiFePO_4$ decreases. The presence of these impurities also affects significantly the electrochemical performance of the material. An evaluation of the performance of the carbon-coated $LiFePO_4$ samples synthesized from different non-stoichiometric proportions over extended constant current charge/discharge cycles for

Table 2 Lattice parameters of $LiFePO_4$ products (based on *Pnma* space group) synthesized from $FePO_4 + x/2Li_2CO_3 + 1/4\,C$ at 1,000 °C and comparison with their electrochemical performance and amount of impurities

x	Capacity (mAh/g)	$Fe_2P_2O_7$ (%)	Li_3PO_4 (%)	a (Å)	b (Å)	c (Å)	V ($Å^3$)	Gof	Rwp	Rp
0.80	118.7	13.6		10.330	6.008	4.692	291.196	2.54	1.85	1.17
0.85	135.1	10.6		10.329	6.004	4.692	290.939	2.96	2.23	1.29
0.90	136.8	5.3		10.336	6.008	4.696	291.620	2.70	1.95	1.17
0.95	143.1	3.4		10.341	6.005	4.694	291.509	2.84	2.09	1.24
1.00	151.1			10.321	6.003	4.693	290.758	3.19	2.15	1.29
1.05	142.9		1.9	10.335	6.010	4.692	291.450	3.18	2.38	1.25
1.10	128.6		6.5	10.323	5.997	4.693	290.490	3.62	2.66	1.38
1.15	97.7		7.8	10.320	6.003	4.691	290.570	2.80	2.11	1.26
1.20	84.2		12.2	10.344	6.014	4.702	292.499	2.44	1.81	1.11

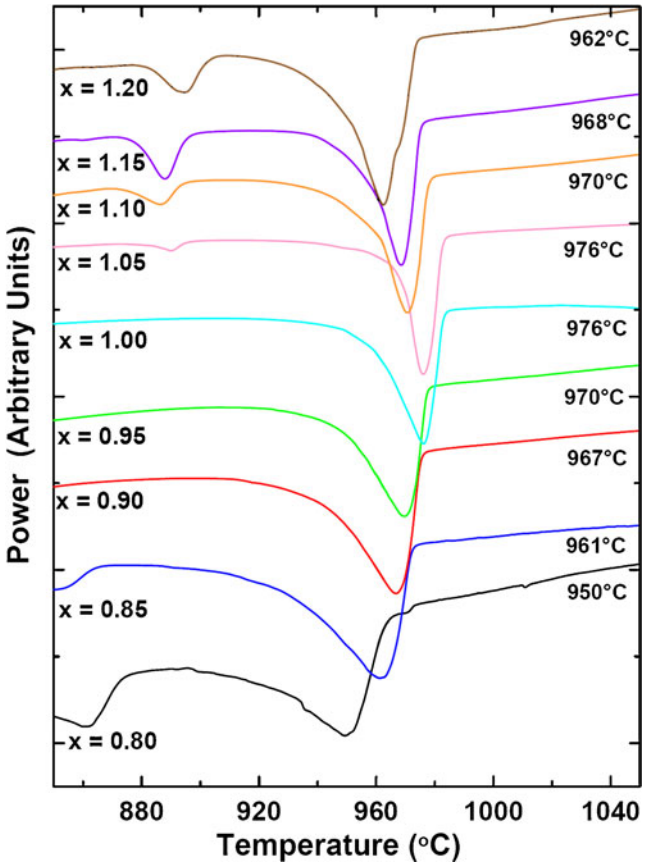

Fig. 7 DSC scan of $LiFePO_4$ products synthesized from $FePO_4 + x/2\,Li_2CO_3 + 1/4C$ at 1,000 °C with the indicated melting point of each sample

the various samples at 25 °C are shown in Fig. 8. Each sample shows good capacity retention over 40 charge/discharge cycles, indicating that an efficient particle size reduction method was used since large particles would have seen a rapid deterioration in performance with increasing cycle life. Large particles are affected more severely by the change in crystallographic volume as they have lower surface area and thus less contact with the polymeric binder than small particles. This leads to greater particle cracking and a loss in electrochemical performance with increasing charge/discharge cycles. The difference in capacities seen between each sample is related directly to the amount of impurities within the samples (Table 2). The sample synthesized with stoichiometric amounts of Li:Fe:P provides the highest capacity, while the further one extends to off-stoichiometric proportions, the lower the electrode capacity. The capacity obtained for the stoichiometric sample is 89% of the theoretical capacity of $LiFePO_4$, and this value compares well with other new synthetic methods (sol gel, polyol) especially since the carbon coating and cell assembly parameters are not optimized in this investigation. In previous work from our laboratory using a more elaborate milling procedure and an optimization of carbon coating, we were able to obtain 95% of theoretical capacity. This indicates that the molten method is a competitive method to other commercial methods for the production of $LiFePO_4$.

Conclusions

To obtain an adequate electrochemical performance from $LiFePO_4$ synthesized from a molten process, an efficient particle size reduction method is required. In this report, we have increased the applicability of the molten approach towards electrode materials through the use of a planetary mill, readily available in most laboratories, as a method of particle size reduction. Milling $LiFePO_4$, using 25 mL of IPA with smaller and smaller milling media, results in a particle size of ~2 μm and a resulting electrode performance of 151 mAh/g (89% of theoretical). There is also improved electrode performance (capacity values and capacity retention) with decreasing particle size of the $LiFePO_4$.

Our first investigation with this milling method has shown that phase-pure $LiFePO_4$ can been synthesized through a stoichiometric combination of Li, Fe, and P precursors, while an off-stoichiometric synthesis results in the formation of either lithium-rich or lithium-poor impurities when the Li precursor combination is changed. The off-stoichiometric combinations result in poor electrochemical performance. In further reports from our group, we will concentrate on expanding the molten synthetic approach to other electrode materials systems.

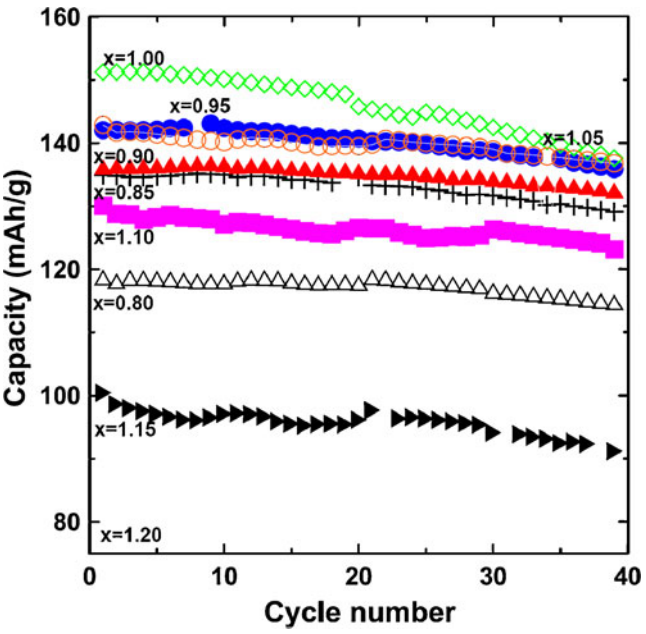

Fig. 8 Discharge capacity versus cycle number of $LiFePO_4$ products synthesized from $FePO_4 + x/2\,Li_2CO_3 + 1/4\,C$ at 1,000 °C at an indicated value of x

Acknowledgements The authors thank NSERC and Phostech Lithium for funding this work under the auspices of the Industrial Research Chair program.

References

1. Linden D (2001) Handbook of batteries, 3rd edn. McGraw-Hill, New York
2. Hatchard TD, MacNeil DD, Basu A, Dahn JR (2001) J Electrochem Soc 148:A755–A761
3. Lombardi C (2006) Sony plans its own battery recall, CNetNews. http://news.cnet.com/Sony-plans-its-own-battery-recall/2100-1044_3-6122234.html?tag=mncol. Accessed 26 Jan 2010
4. MacNeil DD, Dahn JR (2002) J Electrochem Soc 149:A912–A919
5. MacNeil DD, Christiensen L, Landucci J, Paulsen JM, Dahn JR (2000) J Electrochem Soc 147:970–979
6. Padhi AK, Najundaswamy KS, Goodenough JB (1997) J Electrochem Soc 144:1188–1194
7. MacNeil DD, Lu Z, Chen Z, Dahn JR (2002) J Power Sources 108:8–14
8. Armand M, Gauthier M, Magnan JF, Ravet N (2002) WO 02/27823 A1
9. Herle SP, Ellis B, Coombs N, Nazar LF (2004) Nat Mater 3:147–152
10. Yang S, Zavalij PY, Whittingham MS (2001) Electrochem Commun 3:501–508
11. Gauthier M, Michot C, Ravet N, Duchesneau M, Dufour J, Liang G, Wontcheu J, Gauthoer L, MacNeil DD (2010) J Electrochem Soc 157:A453–A462
12. MacNeil DD, Devigne L, Michot C, Rodrigues I, Liang G, Gauthier M (2010) J Electrochem Soc 157:A463–A468
13. Thompson AH (1979) J Electrochem Soc 126:608–616
14. Andersson AS, Kalska B, Haggstrom L, Thomas JO (2000) Solid State Ionics 130:41–52
15. Kang B, Ceder G (2009) Nature 458:190–193
16. Zaghib K, Goodenough JB, Mauger A, Julien C (2009) J Power Sources 194:1021–1023
17. Ceder G, Kang B (2009) J Power Sources 194:1024–1028